Iterative Lavrentiev regularization for symmetric kernel-driven operator equations: with application to digital image restoration problems

WANG Yanfei[1,2], GU Xingfa[1,4], YU Tao[1] & FAN Shufang[3]

1. Institute of Remote Sensing Applications, Chinese Academy of Sciences, Beijing 100101, China;
2. Department of Mathematics, University of Center Florida, FL 32816, USA;
3. Department of Mathematics, Beijing Normal University, Beijing 100875, China;
4. INRA-Unitè de Bioclimatologie 84914, Avignon, France

Correspondence should be addressed to Wang Yanfei (email: yfwang@irsa.ac.cn)

Received January 20, 2005

Abstract The symmetric kernel-driven operator equations play an important role in mathematical physics, engineering, atmospheric image processing and remote sensing sciences. Such problems are usually ill-posed in the sense that even if a unique solution exists, the solution need not depend continuously on the input data. One common technique to overcome the difficulty is applying the Tikhonov regularization to the symmetric kernel operator equations, which is more generally called the Lavrentiev regularization. It has been shown that the iterative implementation of the Tikhonov regularization can improve the rate of convergence. Therefore in this paper, we study the iterative Lavrentiev regularization method in a similar way when applying it to symmetric kernel problems which appears frequently in applications, say digital image restoration problems. We first prove the convergence property, and then under the widely used Morozov discrepancy principle(MDP), we prove the regularity of the method. Numerical performance for digital image restoration is included to confirm the theory. It seems that the iterated Lavrentiev regularization with the MDP strategy is appropriate for solving symmetric kernel problems.

Keywords: Lavrentiev regularization, iterative implementation, discrepancy principle, image restoration.

DOI: 10.1360/122004-176

1 Introduction

In mathematical physics and problems of remote sensing, we are often faced with the inversion of the operator equation

$$Af = g, \tag{1}$$

or

$$\int_\Omega k(x,y)f(y)dy = g(x), \tag{2}$$

where A is the operator mapping $f \in D(f) \subset F$ into G. The operator (1) is usually the first kind of Fredholm integral equation (2). In (2), $k(x,y)$ is the kernel which is a nondegenerate square integrable function and $g(\cdot)$ is a known function, usually the observation. In remotely sensed image processing and atmospheric turbulence, the kernel $k(\cdot,\cdot)$ is usually a point spread function (PSF) or more generally a modulation transfer function (MTF), which is sometimes symmetric, that is $k(x,y)=k(y,x)$; hence the operator A itself is a self-adjoint positive semi-definite operator. Examples for this kind of kernel are some diffraction limited aperture, statistical Gaussian filter, and so on[1,2]. In the following context, we will give some investigation on the symmetric kernel operator equation (1). Without loss of generality, we also assume that A is symmetric semi-definite. Otherwise, (1) can be replaced by

$$A^2 f = Ag. \tag{3}$$

Then A^2 is symmetric semi-definite, and Ag serves as the new right-hand side.

Even for the symmetric semi-definite kernel operator equation (1), it is still ill-posed[3]. This is because the r.h.s. g of (1) usually represents observations, so g may not belong to the range of A. Moreover, g is usually contaminated with noise. Small perturbation in the r.h.s. g will lead to large oscillation of the solution[4−6]. Tikhonov regularization can be employed to solve the symmetric operator equation (1), which is usually called the Lavrentiev regularization, i.e. instead of (1) we solve a well-posed problem

$$Af^\alpha + \alpha f^\alpha = g, \tag{4}$$

where $\alpha > 0$ is called the regularization parameter. It is shown by Schock in ref. [7] that the optimal convergence rate $\|f - f^\alpha\| = O(\alpha^\nu)$ can be satisfied provided that the smooth condition $f \in R(A^\nu),\ \nu \in (0,1]$ is satisfied. The Lavrentiev regularization is generally introduced for solving Volterra integral equations of the first kind[8,9].

For application problems, the r.h.s. g cannot be obtained exactly, and instead one may have g_δ such that

$$\|g_\delta - g\| \leqslant \delta < \|g_\delta\|$$

and $g_\delta \longrightarrow g$ as $\delta \longrightarrow 0$. In such a case, the Lavrentiev regularization should be in the form

$$Af_\delta^\alpha + \alpha f_\delta^\alpha = g_\delta, \tag{5}$$

where α is dependent on the error level δ and satisfies $\alpha(\delta) \longrightarrow 0$ and $f_\delta^\alpha \longrightarrow f$ as $\delta \longrightarrow 0$. Furthermore if we know some smooth condition $f \in R(A^\nu),\ \nu \in (0,1]$, then the optimal convergence rate of asymptotic order $\|f - f_\delta^\alpha\| = O(\delta^{\frac{\nu}{\nu+1}})$ can be satisfied.

It has been shown that the iterative version of the Tikhonov regularization can improve the rate of convergence[10,11]. In ref. [10], the authors use iterative Tikhonov regularization to approximate the generalized inverse of the operator, while the latter is known as the generalized inverse method for ill-posed problems[12] ; in ref. [11], based on the Morozov's discrepancy principle, the authors prove the optimality of the iterative Tikhonov regularization. In ref. [13], the authors consider the non-stationary iterative Tikhonov regularization and prove the optimality. The iterative Lavrentiev regularization has been considered for solving Volterra integral equations of the first kind[14], and applications to the non-destructive testing of optical-fibre preforms are included. Accordingly, in this paper, we will discuss the iterative Lavrentiev regularization methods for symmetric kernel operator equation (1):

$$(A+\alpha I)f_k = \alpha f_{k-1} + g, \ \ k = 1, 2, \cdots, \tag{6}$$

$$f_0 \text{ be given}, \tag{7}$$

where $\alpha > 0$ is given as an apriori, and A is assumed to be a symmetric positive semi-definite operator. The convergence properties for both noise-free case and perturbed case are considered.

2 Convergence properties for exact data

Note that (6)–(7) can be rewritten as

$$f_k = (A+\alpha I)^{-1}g + \alpha(A+\alpha I)^{-1}f_{k-1}, \tag{8}$$

$$f_0 \text{ be given}. \tag{9}$$

By induction for $k = 1, 2, \cdots$, the iteration process can be written in a simple form:

$$f_k = P_{k,\alpha}(A)g + Q_{k,\alpha}(A)f_0, \tag{10}$$

where $P_{k,\alpha}(t)$ and $Q_{k,\alpha}(t)$ are generating functions (for more examples, please see refs. [4, 11]) in the form

$$P_{k,\alpha}(t) = \frac{1}{t}(1 - Q_{k,\alpha}(t)), \tag{11}$$

$$Q_{k,\alpha}(t) = \left(\frac{\alpha}{\alpha+t}\right)^k. \tag{12}$$

It is clear that

$$\|Q_{k,\alpha}(A)\| \leqslant 1$$

and if the inverse of A exists,

$$P_{k,\alpha}(A) \longrightarrow A^{-1} \text{ as } k \longrightarrow \infty.$$

Hence if A^{-1} exists, then $f_k \longrightarrow \hat{f} \overset{def}{=} A^{-1}g$ as $k \longrightarrow \infty$.

Now let $\hat{f}$ be any one solution of $Af = \mathcal{P}g$, where $\mathcal{P}$ is an orthogonal projection of G onto $\overline{R(A)}$. Note that the initial iterate f_0 is given by users. Therefore we can choose $f_0 = 0$. In this way, we have

$$\begin{aligned}\hat{f} - f_k =& \hat{f} - P_{k,\alpha}(A)g - Q_{k,\alpha}(A)f_0\\ =& \hat{f} - P_{k,\alpha}(A)A\hat{f}\\ =& (I - P_{k,\alpha}(A)A)\hat{f}.\end{aligned} \tag{13}$$

It can be seen that $Q_{k,\alpha}(t) = 1 - tP_{k,\alpha}(t) < 1$. Therefore

$$\hat{f} - f_k = Q_{k,\alpha}(A)\hat{f} \tag{14}$$

and

$$\|\hat{f} - f_k\| = \|Q_{k,\alpha}(A)\hat{f}\|. \tag{15}$$

Furthermore, if we know some apriori information about the solution $\hat{f}$, say the smoothing condition about $\hat{f}$: $\hat{f} \in R(A^\nu) \subset N(A)^\perp,\ \nu > 0$, the optimal convergence rate of asymptotic order can be achieved. The convergence analysis will hinge on an investigation of the function

$$\Gamma(t) = t^\nu \left(\frac{\alpha}{t+\alpha}\right)^k.$$

As we are interested in fixed $\nu > 0$ and $k \to \infty$, we shall assume $k > \nu$. Also without loss of generalily, we assume that $\|A\| \leqslant 1$. An easy calculation shows that $\Gamma(t)$ can be maximized if and only if $t = t^*$, where

$$t^* = \frac{\nu}{k-\nu}\alpha.$$

Hence the maximum value of $\Gamma(t)$ is

$$\Gamma_{\max}(t) = \Gamma(t^*) = \nu^\nu \left(\frac{\alpha}{k-\nu}\right)^\nu \left(\frac{k-\nu}{k}\right)^k. \tag{16}$$

Theorem 2.1. Assume that $\hat{f} \in R(A^\nu),\ k > \nu > 0$, then $\|\hat{f} - f_k\| \leqslant C_\nu \nu^\nu (\frac{\alpha}{k})^\nu$.

Proof. Since $\hat{f} \in R(A^\nu)$, and $\nu > 0$, there exists a normalized function $f \in N(A)^\perp$ such that $\hat{f} = A^\nu f$. From (15) and (16), we obtain

$$\begin{aligned}\|\hat{f} - f_k\| =& \|Q_{k,\alpha}(A)A^\nu f\| \\ \leqslant& \nu^\nu \left(\frac{\alpha}{k-\nu}\right)^\nu \left(\frac{k-\nu}{k}\right)^k \\ \leqslant& C_{1,\nu}\nu^\nu \left(\frac{\alpha}{k-\nu}\right)^\nu \\ \leqslant& C_{2,\nu}\nu^\nu \left(\frac{\alpha}{k}\right)^\nu,\end{aligned} \tag{17}$$

where $C_{1,\nu}$ and $C_{2,\nu}$ are two constants related to ν. Let $C_\nu \overset{def}{=} C_{2,\nu}$. This proves the theorem. Q.E.D.

Corollary 2.2. Under the condition of Theorem 2.1, we have

$$\|\hat{f} - f_k\| = O(k^{-\nu}). \tag{18}$$

Furthermore, the "O" estimate in (18) cannot be improved to "o" estimate.

Proof. It is clear from Theorem 2.1 that $\|\hat{f} - f_k\| = O(k^{-\nu})$. Now we prove the "O" cannot be replaced with "o". Instead we suppose that

$$\max \Gamma_{t\in[0,\infty)}(t) \overset{def}{=} t^\nu \left(\frac{\alpha}{t+\alpha}\right)^k = o(k^{-\nu}),\ k \longrightarrow \infty.$$

By Bernoulli's inequality, we have

$$\begin{aligned}\Big(\frac{\alpha}{t+\alpha}\Big)^k =& \Big(1 - \frac{t}{t+\alpha}\Big)^k \\ \geqslant& 1 - \frac{kt}{t+\alpha}.\end{aligned}$$

Choosing $t = k^{-1}$, we obtain

$$1 - \frac{1}{k^{-1} + \alpha} \leqslant k^{\nu} \max_{t \in [0,\infty)} \Gamma(t) = o(1),\ k \longrightarrow \infty,$$

which is a contradiction. Q.E.D.

3 Regularity for inexact data

In this section we consider the perturbed case. We assume that the r.h.s. g is contaminated with noise, i.e. we have g_δ and instead of (6)–(7), we have

$$(A + \alpha I) f_k^\delta = \alpha f_{k-1}^\delta + g_\delta,\ k = 1, 2, \cdots, \tag{19}$$

$$f_0^\delta \text{ be given.} \tag{20}$$

By setting $f_0^\delta = 0$, the iterates f_k^δ can be generated in the following way:

$$f_k^\delta = P_{k,\alpha}(A) g_\delta. \tag{21}$$

Suppose $\|g_\delta - g\| \leqslant \delta$. We now derive a stability estimate for the approximation f_k. Note that

$$1 - tP_{k,\alpha}(t) = Q_{k,\alpha}(t),$$

$$Q_{k,\alpha}(0) = 1.$$

We have by the convexity of $Q_{k,\alpha}(t)$

$$\frac{1 - Q_{k,\alpha}(t)}{t} = \frac{Q_{k,\alpha}(0) - Q_{k,\alpha}(t)}{0 - t} \leqslant -Q'_{k,\alpha}(0).$$

It can be easily computed that $Q'_{k,\alpha}(0) = -k/\alpha$. Thus

$$P_{k,\alpha}(t) \leqslant k/\alpha. \tag{22}$$

Since $f_k,\ f_k^\delta \in D(A)$, we have by (8)–(9), (19)–(20) and (22) that

$$\|f_k - f_k^\delta\| \leqslant \|P_{k,\alpha}(A)(g - g_\delta)\| \leqslant \delta \cdot k/\alpha. \tag{23}$$

Therefore, a sufficient condition for the regularity of the approximations is that the iteration index be chosen in terms of the error level, say $k = k(\delta)$, such that the following condition

$$\delta \cdot k(\delta) \longrightarrow 0 \quad \text{as} \quad \delta \longrightarrow 0 \tag{24}$$

is satisfied. As a consequence, we derive the following

Theorem 3.1. Let $\|g_\delta - g\| \leqslant \delta$ and the iteration index $k = k(\delta)$ be chosen such that $k(\delta) \longrightarrow \infty$ and (24) is satisfied as $\delta \longrightarrow 0$. Then we have the regularity results: $\|f_{k(\delta)}^\delta - \hat{f}\| \longrightarrow 0$ as $\delta \longrightarrow 0$.

Proof. By (15), (23) and noting that the following inequality

$$\|f_{k(\delta)}^\delta - \hat{f}\| \leqslant \|f_k - \hat{f}\| + \|f_k - f_{k(\delta)}^\delta\|,$$

the result is clear. Q.E.D.

Next we establish the optimal convergence rate of asymptotic order for the iterates $\{f_k^\delta\}$ if some priori information of the solution $\hat{f}$, say the smoothing condition, is provided.

Theorem 3.2. Let $\|g_\delta - g\| \leqslant \delta$. Assume that $\hat{f} \in R(A^\nu),\ \nu > 0$. If we choose the iteration index $k = k(\delta)$ in such an apriori way:

$$k(\delta) = \alpha \cdot \delta^{-\frac{1}{\nu+1}},$$

then

$$\|\hat{f} - f^\delta_{k(\delta)}\| \leqslant D_\nu \delta^{\frac{\nu}{\nu+1}}, \tag{25}$$

where D_ν is a constant with respect to ν.

Proof. By Theorem 2.1, Theorem 3.1 and note that the triangular inequality

$$\begin{aligned}\|f^\delta_{k(\delta)} - \hat{f}\| &\leqslant \|f_k - \hat{f}\| + \|f_k - f^\delta_{k(\delta)}\|\\ &\leqslant C_\nu \nu^\nu \left(\frac{\alpha}{k(\delta)}\right)^\nu + \delta \cdot \frac{k(\delta)}{\alpha}\\ &\leqslant (1 + C_\nu \nu^\nu)\delta^{\frac{\nu}{\nu+1}}\\ &= D_\nu \delta^{\frac{\nu}{\nu+1}},\end{aligned}$$

where $D_\nu = 1 + C_\nu \nu^\nu$. Q.E.D.

From Theorem 3.2 we know that the optimal order of convergence is obtained if the choice of $k(\delta)$ is in an apriori way, i.e. $k(\delta) = \alpha \cdot \delta^{-\frac{1}{\nu+1}}$. Both the iteration index k and the parameter α serve as the regularization parameters. However, this is not applicable in applications. In practice, a posteriori way will be better. A popular posteriori way is the discrepancy principle: the iteration process should be stopped at the first occurrence of the index $k(\delta)$ such that

$$\|Af^\delta_{k(\delta)} - g_\delta\| \leqslant \tau\delta \tag{26}$$

with $\tau > 1$ another parameter.

In the following we will analyze that the iteration with the discrepancy principle as the stopping rule is a regularization.

Theorem 3.3. If $k(\delta)$ is chosen by the above stopping rule, then

$$\|g - Af_{k(\delta)}\| \leqslant (\tau + 1)\delta, \tag{27}$$

$$\|g - Af_{k(\delta)-1}\| > (\tau - 1)\delta. \tag{28}$$

Moreover, the discrepancy principle (26) will terminate the iteration after $k(\delta) < \infty$ iterations.

Proof. Note that $Q_{k,\alpha}(t) \leqslant 1$ and

$$g - Af_{k-1} = g_\delta - Af^\delta_{k-1} - Q_{k,\alpha}(A)(g_\delta - g)$$

and

$$g - Af_k = g_\delta - Af^\delta_k + Q_{k,\alpha}(A)(g - g_\delta),$$

so let $k = k(\delta)$ and by triangular inequalities. We have

$$\begin{aligned}\|g - Af_{k(\delta)-1}\| &= \|g_\delta - Af^\delta_{k(\delta)-1} - Q_{k(\delta)-1,\alpha}(A)(g_\delta - g)\|\\ &\geqslant \|g_\delta - Af^\delta_{k(\delta)-1}\| - \|Q_{k(\delta)-1,\alpha}(A)(g_\delta - g)\|\\ &\geqslant \tau\delta - \delta = (\tau - 1)\delta;\end{aligned}$$

$$\begin{aligned}\|g-Af_{k(\delta)}\| =&\|g_\delta - Af^\delta_{k(\delta)} + Q_{k(\delta),\alpha}(A)(g-g_\delta)\|\\ \leqslant&\|g_\delta - Af^\delta_{k(\delta)}\| + \|Q_{k(\delta),\alpha}(A)(g-g_\delta)\|\\ \leqslant&\tau\delta+\delta=(\tau+1)\delta.\end{aligned}$$

Furthermore, note that $Q_{k,\alpha}(t) \longrightarrow 0$ as $k \longrightarrow \infty$. Hence the discrepancy $g_\delta - Af^\delta_{k(\delta)}$ satisfies

$$\begin{aligned}\|g_\delta - Af^\delta_{k(\delta)}\| =&\|g_\delta - AP_{k(\delta),\alpha}(A)g_\delta\|\\ =&\|Q_{k(\delta),\alpha}(A)g_\delta\|\\ \leqslant&\epsilon,\end{aligned}$$

where ϵ is an arbitrarily small number. This indicates that the discrepancy principle (26) will terminate the iteration after $k(\delta)<\infty$ iterations. Q.E.D.

Theorem 3.4. Assume that $\hat f \in R(A^\nu),\ \nu>0$, $f^\delta_{k(\delta)}$ is the solution of (1) when y_δ instead of y is given and $k(\delta)$ is chosen according to (26). Then $\|f^\delta_{k(\delta)} - \hat f\| = O(\delta^{\frac{\nu}{\nu+1}})$.

Proof. Suppose $\hat f = A^\nu z$, where z is normalized and $z\in R(A^\nu),\ \nu>0$. Then

$$f_{k(\delta)} - \hat f = Q_{k(\delta),\alpha}(A)A^\nu z.$$

By Hölder's inequality and (27) of Theorem 3.3, we have the estimate

$$\begin{aligned}\|f_{k(\delta)} - \hat f\| \leqslant&\|Q_{k(\delta),\alpha}(A)z\|^{\frac{1}{\nu+1}}\|AQ_{k(\delta),\alpha}(A)A^\nu z\|^{\frac{\nu}{\nu+1}}\\ \leqslant&\|z\|^{\frac{1}{\nu+1}}\|A(f_{k(\delta)}-\hat f)\|^{\frac{\nu}{\nu+1}}\\ =&O(\delta^{\frac{\nu}{\nu+1}}).\end{aligned}$$

Now assume that $k(\delta)\geqslant \lceil \nu+3\rceil$, by (28) of Theorem 3.3,

$$\begin{aligned}(\tau-1)\delta <&\|g-Af_{k(\delta)-1}\|\\ =&\|AQ_{k(\delta)-1,\alpha}(A)A^\nu z\|.\end{aligned}$$

By (16), we find

$$\begin{aligned}\|AQ_{k(\delta)-1,\alpha}(A)A^\nu z\|^2 =&(A^2Q_{k(\delta)-1,\alpha}(A)A^\nu z, Q_{k(\delta)-1,\alpha}(A)A^\nu z)\\ \leqslant&E_{1,\nu}(\frac{\alpha}{k(\delta)})^{\nu+2}\cdot C_\nu \nu^\nu(\frac{\alpha}{k(\delta)})^\nu\\ =&E_{2,\nu}(\frac{\alpha}{k(\delta)})^{2(\nu+1)},\end{aligned}$$

where $E_{1,\nu}$ and $E_{2,\nu}$ are two constants with respect to ν. Thus

$$(\tau-1)\delta < E_\nu\left(\frac{\alpha}{k(\delta)}\right)^{\nu+1}, \tag{29}$$

where $E_\nu=\sqrt{E_{2,\nu}}$. This shows

$$k(\delta)\leqslant F_\nu\cdot\alpha\delta^{-\frac{1}{\nu+1}}, \tag{30}$$

where $F_\nu = (\frac{E_\nu}{\tau-1})^{\frac{1}{\nu+1}}$. Now by (23), we obtain

$$\|f^\delta_{k(\delta)} - \hat f\| \leqslant O(\delta^{\frac{\nu}{\nu+1}}) + \frac{\delta\cdot F_\nu\cdot\alpha\delta^{-\frac{1}{\nu+1}}}{\alpha}$$

$$= O(\delta^{\frac{\nu}{\nu+1}}). \qquad \text{Q.E.D.}$$

From this theorem we find that at the stopping index, $\frac{k(\delta)}{\alpha} = O(\delta^{-\frac{1}{\nu+1}})$. Especially when $\alpha \sim \delta$, we have $k(\delta) = O(\delta^{\frac{\nu}{\nu+1}})$, which means $k(\delta) \to O(1)$ as $\nu \to 0$ and $k(\delta) \to O(\delta)$ when ν is sufficiently large.

4 Digital image restoration

4.1 PSF convolution kernel-driven image restoration

This section provides some applications in applied optics and remote sensing sciences. Atmospheric turbulence blur arises in applied optics and remote sensing is due to long-term exposure through the atmosphere where turbulence in the atmosphere gives rise to random variations in the refractive index. A simple forward model for simulating this process is the convolution of the kernel k with the input signal f which results in a smoothing function f:

$$k \star f \stackrel{def}{=} \int_\Omega k(x-y)f(y)dy = g(x). \tag{31}$$

The kernel k is sometimes called the point spread function (PSF). The PSF k is more like a Dirac delta function $\delta(x)$:

$$\begin{cases} \delta(x) = 0, & \text{if} \quad x \in \mathbb{R}\backslash 0, \\ \int_{-\infty}^{\infty} \delta(x) = 1, & \text{else.} \end{cases} \tag{32}$$

The Dirac delta function is symmetric. By shifting property of the delta function, convolving with a delta function does not alter the function f. This is to be expected, since we said convolving f with our choice of kernel k results in smoothing of f, because atmospheric turbulence is hard to predict and can currently only be accessed by statistic process. In atmospheric applications, we usually choose the kernel k as a Gaussian point spread function

$$k(x) = \frac{1}{\sqrt{2\pi}\sigma} \exp\Big(-\frac{1}{2}\Big(\frac{x}{\sigma}\Big)^2\Big), \tag{33}$$

where σ is a positive constant. In two-dimensional cases, the kernel k is in the form

$$k(x,y) = \frac{1}{\sqrt{2\pi}\sigma} \exp\Big(-\frac{1}{2}\Big(\frac{x^2+y^2}{\sigma}\Big)\Big). \tag{34}$$

The larger σ we choose, the more f gets smoothed. So by the same argument, the smaller σ we choose, the more the convolution result resembles f.

Example 4.1. Gaussian kernel-driven image restoration

The PSF kernel is the Gaussian function as in (33). The input signal is a 1d function with two peaks

$$f(x) = 2\exp(-20(x-0.2)^2) + \exp(-80(x-0.8)^2).$$

The interest domain is $\Omega = [0,1] \times [0,1]$. The right-hand side g can be obtained by evaluating the convolution process (31). The inverse problem is recovering the unknown

f by giving the right-hand side g. To numerically restore f, we discretize the domain in both directions. The mesh grid numbers are 100. Both k and f are discretized by collocation. This yields a simple matrix-vector equation

$$\mathcal{A}F = G. \tag{35}$$

The matrix $\mathcal{A}$ is 100×100 and it models Gaussian spatially invariant blur with point spread function k. The plot of the PSF is illustrated in Fig. 1. Small values of A are replaced by zero, and the resulting matrix $\mathcal{A}$ is a banded Toeplitz matrix . The bandwidth we choose is $p = 3$, i.e. only pixels within a distance 2 contribute to the blurring.

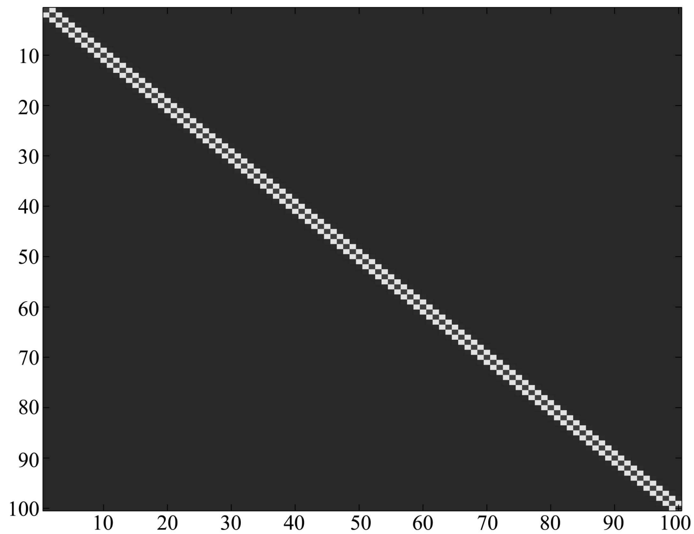

Fig. 1. The Gaussian PSF.

The discretized matrix $\mathcal{A}$ is positive definite, which is illustrated in Fig. 2. Therefore, our method works. To be meaningful, we assume that the right-hand side G is perturbed by additive noise, i.e., instead of G, we would have

$$G_\delta = G + \delta \cdot rand(size(G))$$

and solve the following equation

$$\mathcal{A}F = G_\delta, \tag{36}$$

where $rand(\cdot)$ is the Gaussian white noise having the same dimension as that of g. Then the iteration process reads as

$$F_k^\delta = (\mathcal{A} + \alpha I)^{-1} G_\delta + \alpha(\mathcal{A} + \alpha I)^{-1} F_{k-1}^\delta, \tag{37}$$

$$F_0^\delta = 0. \tag{38}$$

Note that for $\alpha > 0$, $\mathcal{A} + \alpha I$ is always banded symmetric and positive definite. This means that we can use the Cholesky decomposition for solving (37) and (38). For the sake of saving the amount of computation, we apply the Gaxpy Cholesky decomposition, which means

$$\text{vector} \longleftarrow \text{vector} + \text{matrix} \times \text{vector}$$

and

$$\mathcal{A} = D \cdot D^T,$$

where D is lower triangular with the same bandwidth as A. If $N >> p$, then the amount of computation is $O(N^2(p^2 + 3p + 1))$.

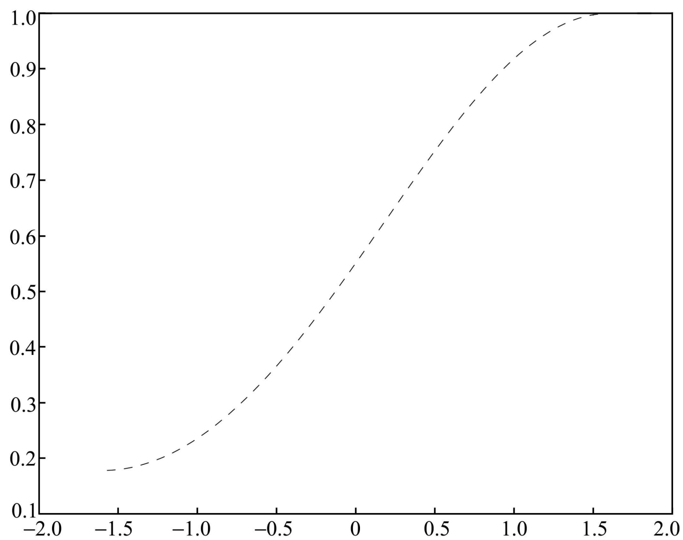

Fig. 2. Eigenvalues of discrete PSF kernel.

By Theorem 3.4, the optimized iteration steps are $k(\delta) = O(\delta^{\frac{\nu}{\nu+1}})$ when $\alpha \sim \delta$. This means that it needs very few steps to generate convergence for given error level $\delta \in (0, 1)$ and any $\nu > 0$. Therefore, by Theorem 3.4, the values of α are chosen as error level δ. The simulation results are shown in Fig. 3. In all of the cases, we choose $\tau = 1.01$. For the first case, it needs 2 steps to reach the convergence with the residual 0.00027212. For the second, it needs 2 steps to reach the convergence with the residual 0.0010836. For the third, it needs 2 steps to reach the convergence with the residual 0.027465.

Example 4.2. Diffraction limited PSF kernel-driven image restoration

The atmospheric image is generated through a simulated diffraction limited PSF with aperture $p(x, y)$ and phase $\phi(x, y)$ convolved with the input $f(x, y)$

$$PSF \star f \stackrel{def}{=} \int_{\Omega} PSF(x - \xi, y - \eta) f(\xi, \eta) d\xi d\eta = g(x, y), \tag{39}$$

where $PSF = |IFT(p(x, y) \exp(i\phi(x, y))|^2$, $IFT(\cdot)$ is the inverse Fourier transform of a function. We also denote $FT(\cdot)$ as the Fourier transform of a function. The simulated PSF is an ideal source light which is plotted in Fig. 4 and the phase ϕ is plotted in Fig. 5.

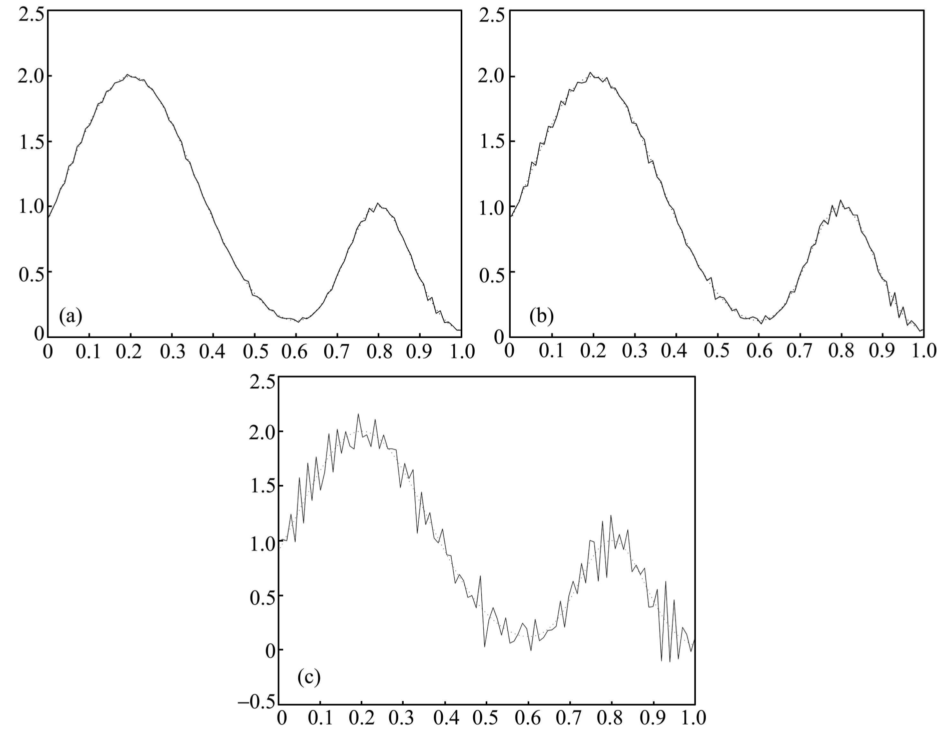

Fig. 3. The true image (dotted line) and restoration image (dashed line) with different error levels: (a) $\delta = 0.005$; (b) $\delta = 0.01$; (c) $\delta = 0.05$.

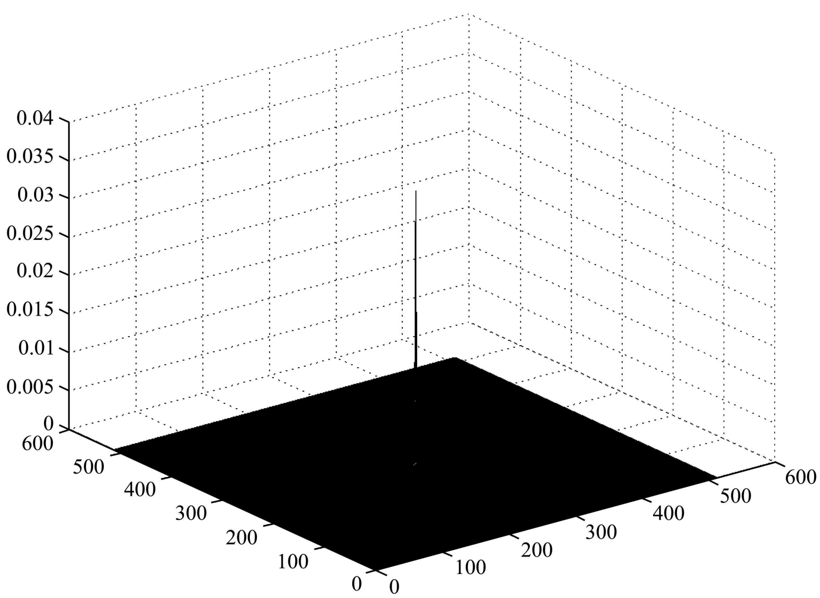

Fig. 4. The diffraction limited point spread function.

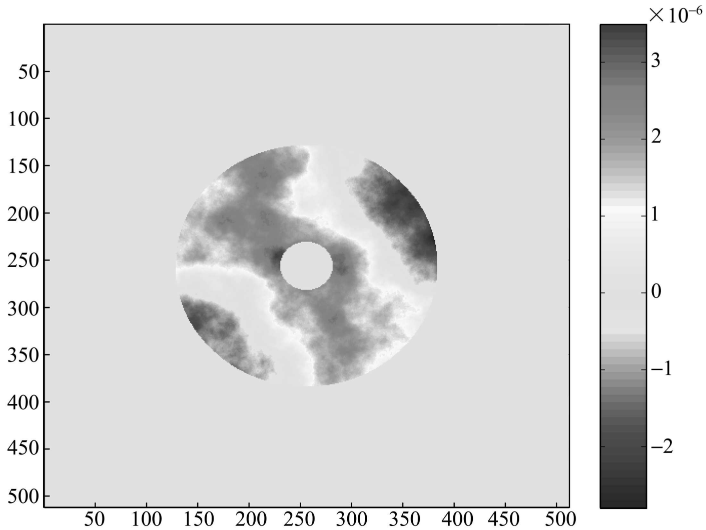

Fig. 5. The phase function.

Note that the phase variation is small in this test to ensure the symmetric, positive semi-definite property of the PSF. Practically, phase can be large. In the latter situation, instead of Lavrentiev regularization, the Tikhonov regularization should be employed. The input function $f(x, y)$ is a farmland whose size is 256-by-256. Therefore, the discrete PSF size is 65536-by-65536. This results in a matrix-vector expression of the convolution (39)

$$\mathcal{A}\mathrm{vec}(F) = \mathrm{vec}(G), \tag{40}$$

where $\mathrm{vec}(\cdot)$ defines a linear mapping which is the lexicographical column ordering of the elements in the given array. The iteration process is as follows:

$$\mathrm{vec}(F)_k^\delta = (\mathcal{A} + \alpha I)^{-1}\mathrm{vec}(G)_\delta + \alpha(\mathcal{A} + \alpha I)^{-1}\mathrm{vec}(F)_{k-1}^\delta, \tag{41}$$

$$\mathrm{vec}(F)_0^\delta = 0. \tag{42}$$

Note that the large size of the matrix and the input, the direct matrix decomposition should be precluded. It is clear that the convolution process can be implemented by 2d fast Fourier transform FFT2 and 2d inverse fast Fourier transform IFFT2. Let us denote

$$\widehat{\mathrm{vec}(F)}_k^\delta = FFT2(\mathrm{vec}(F)_k^\delta),\ \widehat{\mathrm{vec}(G)}_\delta = FFT2(\mathrm{vec}(G)_\delta),$$
$$\hat{\mathcal{A}} = FFT2(\mathcal{A}),\ \hat{I} = FFT2(I).$$

Then

$$\widehat{\mathrm{vec}(F)}_k^\delta = \frac{\widehat{\mathrm{vec}(G)}_\delta + \alpha\widehat{\mathrm{vec}(F)}_{k-1}^\delta}{(|\hat{\mathcal{A}}| + \alpha\hat{I})},$$
$$\mathrm{vec}(F)_k^\delta = IFFT2(\widehat{\mathrm{vec}(F)}_k^\delta).$$

The imposed error level is $\delta = 0.01$. Using our method, it takes 3 steps to generate convergence with the residual 0.0349. See Fig. 6 for the true, noisy and recovered images.

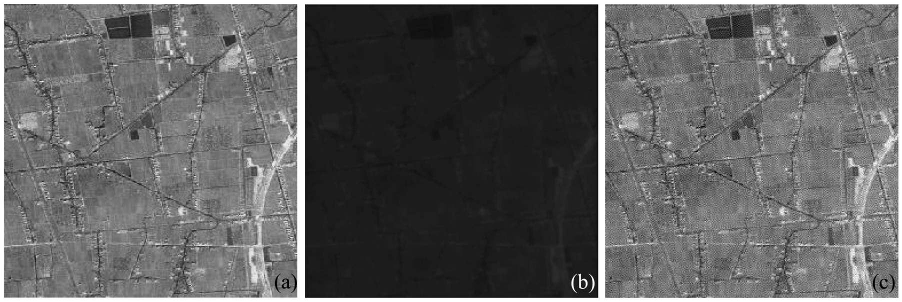

Fig. 6. (a) True image; (b) blurred noisy image; (c) restoration.

4.2 Long slit PSF kernel-driven image restoration

The driven-kernels given in the former subsection are symmetric and positive semi-definite. But not every symmetric kernel-driven equation can be applied directly by the method developed in this paper. It is true that the iteration process can be implemented as long as $A+\alpha I$ is positive definite for choice of large values of α without caring about the negative values of A. However, nonconvergence will occur. For example, the operator $\mathcal{L}$ of the Laplace transform

$$(\mathcal{L}f)(s) = \int_{t_{\min}}^{t_{\max}} \exp(-st)f(t)dt$$

is symmetric but not positive semi-definite in the domain $[0,1]$.

Another example, the infinite long slit PSF can be written as the following function[15]:

$$k(\theta,\phi) = (\cos\theta + \cos\phi)\Big(\frac{\sin r}{r}\Big)^2, \tag{43}$$

where

$$r = \frac{\pi w}{\lambda}(\sin\theta + \sin\phi),$$

θ is the angle of emergence or observation which specifies the location of the image point, ϕ is the angle of incidence which specifies the location of the source, w is the width of the slit, and λ is the wavelength. It is easy to find that the kernel is symmetric. Use similar discretization process as in Example 4.1, we have matrix-vector equation

$$\mathcal{A}F = G. \tag{44}$$

The matrix size of $\mathcal{A}$ is 100-by-100. The plot of the PSF is illustrated in Fig. 7. By eigenvalue decomposition, we plot the eigenvalues in Fig. 8. It is clear that there are many negative eigenvalues occur. Hence the PSF kernel is not semi-definite. To employ the method developed in this paper, we need to transfer (45) into the one

$$\mathcal{A}^2F = \mathcal{A}G. \tag{45}$$

Now the new matrix $\mathcal{A}^2$ is semi-definite. For $\alpha > 0$, $\mathcal{A}^2 + \alpha I$ is positive definite. However, the iteration process (6)–(7) is retraced to Tikhonov regularization if we recognize that $\mathcal{A}^2 = \mathcal{A}^T\mathcal{A}$, i.e.

$$(A^2 + \alpha I)f_k = \alpha f_{k-1} + Ag,\ \ k = 1,2,\cdots, \tag{46}$$

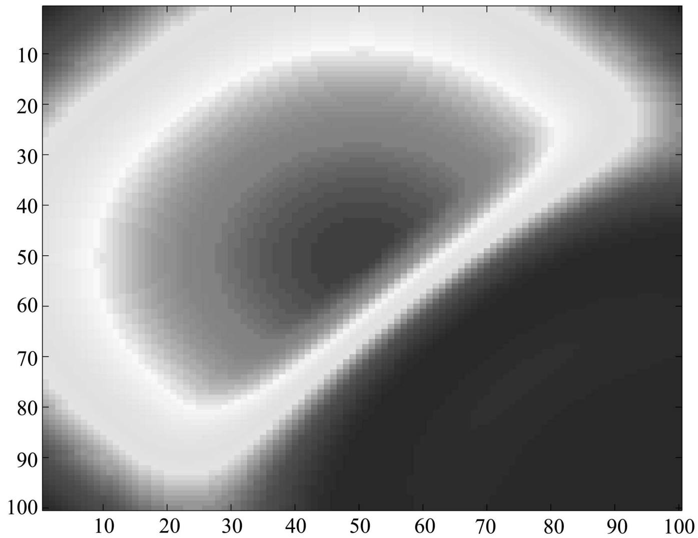

Fig. 7. The long slit PSF.

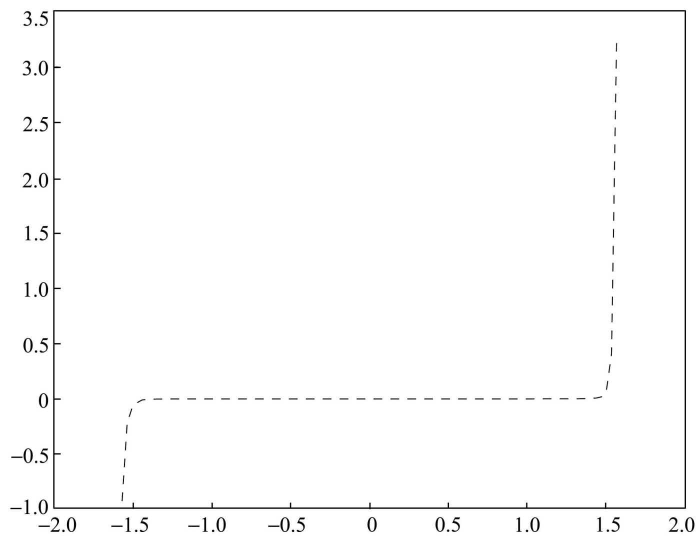

Fig. 8. Eigenvalues of discrete PSF kernel.

$$f_0 \text{ be given.} \tag{47}$$

The input signal is assumed to be the superimposed Gaussian

$$f(\phi) = \exp(-c_1(\phi - \phi_a)^2) + c(-c_2(\phi - \phi_b)^2).$$

Assuming that $\theta,\ \phi \in [-\frac{\pi}{2}, \frac{\pi}{2}]$, we choose $c = 1$, c_1 and c_2 as high as 4, and ϕ_a and ϕ_b as small as $\pm\frac{1}{2}$. The restoration results are shown in Fig. 9. In all cases, we choose $\tau = 1.01$. For the first case, it needs 2 steps to reach the convergence with the residual 0.097774. For the second, it needs 2 steps to reach the convergence with the residual 0.1966. For the third, it needs 2 steps to reach the convergence with the residual 0.95535.

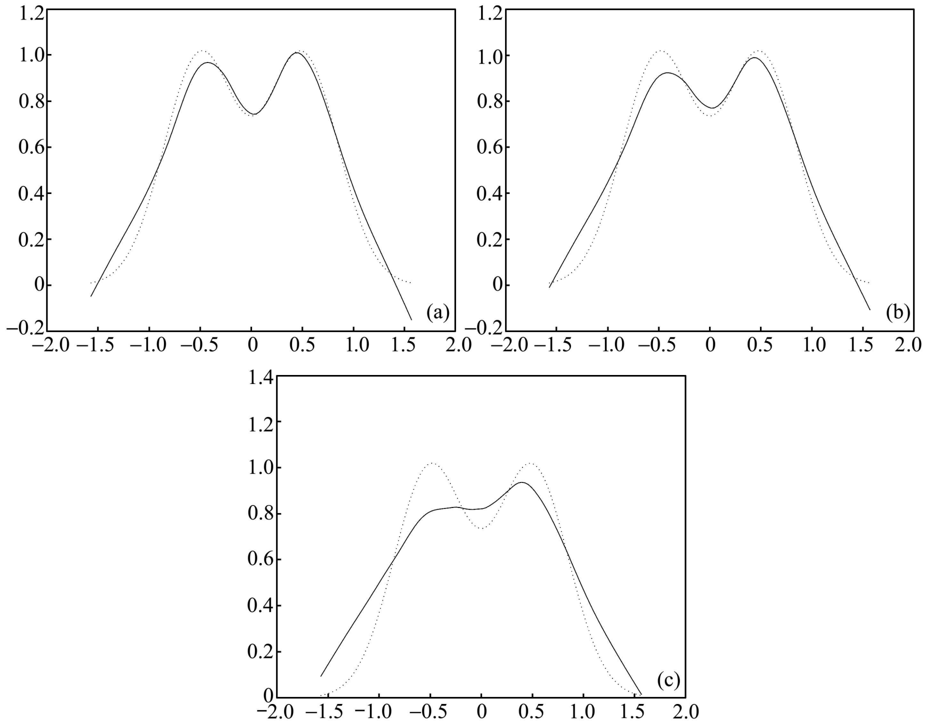

Fig. 9. The true image (dotted line) and restoration image (dashed line) with different error levels: (a) δ=0.005; (b) δ=0.01; (c) δ=0.05.

5 Further extension

We have noted that the iterative formula (6)–(7) can be implemented for non-stationary choice of the regularization parameter α, i.e. instead of choosing fixed $\alpha > 0$, we choose $\alpha := \alpha_k$ and have

$$(A + \alpha_k I)f_k = \alpha_k f_{k-1} + g, \; k = 1, 2, \cdots, \tag{48}$$

$$f_0 \text{ be given.} \tag{49}$$

The regularization parameter α_k can be chosen geometrically[16,17], say

$$\alpha_k = Const. \times \xi^{k-1}, \; \xi \in (0, 1).$$

For the non-stationary iteration formula (48)–(49), and noting that $A\hat{f} = g$, we have

$$f_k = \alpha_k (A + \alpha_k I)^{-1} f_{k-1} + (A + \alpha_k I)^{-1} A\hat{f}. \tag{50}$$

Since

$$I - (A + \alpha_k I)A = \alpha_k (A + \alpha_k I)^{-1},$$

we have

$$\begin{aligned}\hat{f} - f_k =& \hat{f} - \alpha_k(A + \alpha_k I)^{-1} f_{k-1} - (A + \alpha_k I)^{-1} A\hat{f} \\ =& \alpha_k (A + \alpha_k I)^{-1} (\hat{f} - f_{k-1}) \\ =& \cdots \\ =& \prod_{i=1}^{k} \alpha_i (A + \alpha_i)^{-1} \hat{f}.\end{aligned}$$

Hence

$$f_k = \hat{f} - \prod_{i=1}^{k} \alpha_i (A + \alpha_i)^{-1} \hat{f} = \Gamma(A)\hat{f}, \tag{51}$$

where $\Gamma(\cdot)$ is the filter function, which is in the form

$$\Gamma(t) = 1 - \prod_{i=1}^{k} \frac{\alpha_i}{t + \alpha_i}.$$

It is clear that

$$\begin{aligned}&\Gamma(t) \longrightarrow 1 \quad \text{as} \quad \alpha_i \longrightarrow 0, \quad i \longrightarrow \infty \\ &\Gamma(t) \longrightarrow 0 \quad \text{as} \quad t \longrightarrow 0.\end{aligned}$$

This indicates that $\Gamma(A)$ is a suitable approximation to the identity. Thus the iteration process is convergent. Let us denote

$$\gamma_k(t) = \prod_{i=1}^{k} \frac{\alpha_i}{t + \alpha_i}.$$

Then

$$\Gamma(t) = 1 - \gamma_k(t) \quad \text{and} \quad \hat{f} - f_k = \gamma_k(A)\hat{f}.$$

Under the smoothing condition about $\hat{f}$: $\hat{f} \in R(A^\nu) \subset N(A)^\perp,\ \nu > 0$, we have

$$\hat{f} - f_k = \Phi_\nu(A) w \stackrel{def}{=} \gamma_k(A) A^\nu w, \tag{52}$$

with

$$\Phi_\nu(t) = \gamma_k(t) t^\nu = t^\nu \prod_{i=1}^{k} \frac{\alpha_i}{t + \alpha_i}.$$

Now both the convergence and regularity results can be obtained by similar discussion as in ref. [13].

6 Concluding remarks

We have developed an iterative method for the implementation of the Lavrentiev regularization for the semi-definite symmetric kernel operator equations. This method is an extension of the iterative Tikhonov regularization method. However, it is meaningful to study this kind of problem with the special structure/symmetric kernel due to its importance to practical applications. It seems from the theoretical analysis and computational results that the iterative Lavrentiev regularization is appropriate for digital image restoration when the model is semi-definite and symmetric.

Acknowledgements This work was partially supported by the Scientific Research Foundation for the Returned Overseas Chinese Scholars, State Education Ministry.

References

1. Roggemann, M. C., Welsh, B., Imaging Through Turbulence, New York: CRC Press, 1996.
2. Bertero, M., Boccacci, P., Introduction to Inverse Prolems in Imaging, Bristol: IOP Publishing, 1998.
3. George, S., Nair, M. T., A class of discrepancy principles for the simplified regularization of ill-posed problems, J. Austral. Math. Soc., Ser. B, 1994, 36: 242–248.
4. Groetsch, C. W., The Theory of Tikhonov Regularization for Fredholm Equations of the First Kind, Pitman Advanced Publising Program, 1984.
5. Engl, H. W., Hanke, M., Neubauer, A., Regularization of Inverse Problems, Dordrecht: Kluwer, 1996.
6. Xiao, T. Y., Yu, S. G., Wang, Y. F., Numerical Methods for Inverse Problems (in Chinese), Beijing: Science Press, 2003.
7. Schock, E., On the asymptotic order of accuracy of Tikhonov regularization, J. Optim. Theory Appl., 1984, 44: 95–104.
8. Corduneanu, C., Integral Equations and Applications, Cambridge: Cambridge University Press, 1991.
9. Plato, R., Iterative and Parametric Methods for Linear Ill-posed Problems, TU Beilin: Habiliationsschrift Fachbereich Mathematik, 1995.
10. King, J. T., Chillingworth, D., Approximation of generalized inverses by iterated regularization, Numer. Funct. Anal. Optim., 1979, 1: 499–513.
11. He, G. Q., Liu, L. X., A kind of implicit iterative methods for ill-posed operator equations, Journal of Computational Mathematics, 1999, 17: 275–284.
12. Nashed, M. Z., Generalized Inverse and Applications, New York: Academic Press, 1976.
13. Hanke, M., Groetsch, C. W., Nonstationary iterated Tikhonov regularization, Journal of Optimization Theory and Applications, 1998, 98: 37–53.
14. Plato, R., Lavrentiev's method for linear Volterra integral equations of the first kind, with applications to the nondestructive testing of optical-fibre preforms, Inverse Problems in Medical Imaging and Nondestructive Testing (Oberwolfach, 1996), Vienna: Springer, 1997, 196–211.
15. Shaw, C. B. Jr., Improvement of the resolution of an instrument by numerical solution of an integral equation, J. Math. Anal. Appl., 1972, 37: 83–112.
16. Tikhonov, A. N., Arsenin, V. Y., Solutions of Ill-Posed Problems, New York: Wiley, 1977.
17. Hofmann, B., Regularization for Applied Inverse and Ill-posed Problems, Leipzig: Teubner, 1986.